Functional & Integrative Genomics (2025) 25:36
https://doi.org/10.1007/s10142-025-01545-w

RESEARCH

TFAP2A-regulated CRNDE enhances colon cancer progression and chemoresistance via RIPK3 interaction

Xin Gao[1] · Yanming Huang[1] · Tonghui Wei[1] · Jingmin Xue[1] · Filippov Iurii[1,2] · Laishou Yang[1] · Liying Wang[1] · Hao Li[1] · Genshen Mo[1] · Yuze Huang[1] · Haonan Xie[1] · Hang Wang[1] · Shenghan Lou[1] · Peng Han[1,3]

Received: 6 October 2024 / Revised: 12 December 2024 / Accepted: 27 January 2025

Abstract
Colon cancer (CC) is a common malignancy with rising incidence worldwide. Despite advances in treatment strategies, many patients still face a poor prognosis due to the development of drug resistance. Long non-coding RNAs (lncRNAs) have emerged as important regulators of various biological processes and have been implicated in cancer progression. Among them, colorectal neoplasia differentially expressed (CRNDE) has drawn attention for its potential roles in different cancers. However, its specific functions in CC remain unclear. In this study, we identified CRNDE as highly expressed in CC, contributing to tumor progression and drug resistance. Mechanically, CRNDE is regulated by the transcription factor TFAP2A. Additionally, CRNDE inhibits pyroptosis, a form of programmed cell death, by promoting the ubiquitin-mediated degradation of RIPK3, thereby reducing the sensitivity of CC cells to 5-fluorouracil (5-FU). Our findings suggest that the TFAP2A/CRNDE/RIPK3 axis plays critical roles in colon cancer progression and chemoresistance, highlighting potential therapeutic targets for improving treatment outcomes.

Keywords Colon cancer · CRNDE · RIPK3 · TFAP2A · Pyroptosis · 5-FU

Introduction

Colon cancer (CC) is type of malignant tumor originating from colon epithelial cells, with increasing incidence in recent years, and has become the important public health challenge in developing countries (Brenner et al. 2021). Although the application of multi-drug combination chemotherapy, targeted therapy and immunotherapy has improved the prognosis of some patients, issues such as drug resistance, non-specific targeting, and dose-dependent toxicity limit the effectiveness of these treatments, thus the survival benefit and the prognostic situation at the population level remain unfavorable (Fenocchio 2024; Ma et al. 2021). To improve the diagnosis and treatment of CC, we urgently need to study the pathogenesis and drug resistance mechanism of CC, and find precise, efficient and individualized intervention targets.

Long non-coding RNAs (lncRNAs) were previously thought to be "noise" in genomic transcripts (Slack et al. 2019). With advances in genomics research in recent years, lncRNAs have gradually been recognized as important regulators of biological processes, that can participate in the occurrence and development of diseases by regulating key processes such as cell differentiation, autophagy and apoptosis (Chen et al. 2022; Matsui et al. 2017; Wei et al. 2024). In the field of tumor research, certain lncRNAs reshape the tumor immune microenvironment by regulating ferroptosis, antigen presentation, and other mechanisms, thereby mediating tumor resistance to immunotherapy or targeted therapy (Chen et al. 2024; Li et al. 2024; Yao et al. 2024). Therefore, lncRNAs are being explored as potential molecular targets for developing novel anti-tumor therapeutic strategies.

In recent years, studies have revealed that the lncRNA CRNDE is abnormally highly expressed and plays pivotal

Xin Gao, Yanming Huang and Tonghui Wei contributed equally to this work and should be considered as co-first authors

✉ Peng Han
leospiv@hrbmu.edu.cn

[1] Department of Oncology Surgery, Harbin Medical University Cancer Hospital, Harbin, China

[2] Bashkir State Medical University, Ufa 450008, Russia

[3] Key Laboratory of Tumor Immunology in Heilongjiang, Harbin, China

Published online: 15 February 2025

roles in various human malignant tumors, including lung adenocarcinoma, oral cancer, renal clear cell carcinoma, and glioma (Chen et al. 2016; Ding et al. 2022; Gu et al. 2024; Shao et al. 2016; Tang et al. 2018; Wang et al. 2015, 2022; Yu et al. 2021; Zhu et al. 2021). However, the role of CRNDE in CC remains unclear.

TFAP2A, member of transcription factor, has garnered attention for its pronounced roles in several human malignancies. Elevated expression levels of TFAP2A have been consistently documented and associated with the progression of tumors (Liu et al. 2023; Ma et al. 2016; Schulte et al. 2008; Zou et al. 2024).

RIPK3 is the serine/threonine protein kinase belonging to the receptor-interacting protein (RIP) family that plays key roles in cell signaling. In oncology research, RIPK3 has attracted significant attention because of its involvement in various cancer-related processes. It also serves as component of the TNF receptor-I signaling complex and can induce pyroptosis, a form of programmed cell death (Babcook et al. 2014; Cho et al. 2018; Conev et al. 2019; Duangthim et al. 2024; Liang et al. 2024).

This study is the first to report the aberrant expression of CRNDE in CC and its close association with tumor development. Mechanistically, CRNDE is positively regulated by TFAP2A, and inhibits the pyroptosis process by promoting the ubiquitin-mediated degradation of RIPK3, thereby enhancing tumor progression and diminishing its sensitivity to 5-fluorouracil (5-FU).

Methods

Bioinformatics analysis

We utilized datasets including TCGA-COAD, GSE84983, GSE110715, GSE117830, GSE146009, and GSE180440 to conduct comprehensive bioinformatics analysis to explore the molecular characteristics of CC. First, the RNA-seq data were normalized, and differential expression analysis was carried out. The core genes were visualized through Venn diagrams, heatmaps, and volcano diagrams. To further investigate the role of CRNDE in regulating CC development, we classified patients into high- and low-expression groups based on the median expression level of CRNDE. We then identified dysfunctional signaling pathways in CC through gene set enrichment analysis (GSEA) and utilized R language packages, including Pathview and Circos, to visualize the corresponding data. For the upstream regulatory mechanism of CRNDE, we used databases such as UCSC (https://genome.ucsc.edu/) and JASPAR (https://jaspar.elixir.no/) to predict potential transcription factors for CRNDE.

Cell culture and transfection

RKO and LoVo were stored in our laboratory. Cells were cultured in complete medium containing 10% fetal bovine serum (FBS) and maintained at 37 °C and 5% CO_2 with regular media changes. RKO and LoVo cells were respectively transfected with shRNA and the CRNDE overexpression plasmid (Invitrogen, USA) respectively. The cells were seeded in 6-well plates on the day prior to transfection to ensure a cell density of 70–80%. For shRNA transfection, the plasmid was first diluted proportionally with Lipofectamine 2000 (Invitrogen) in serum-free medium then incubated to form complexes. After transfection, qRT-PCR was used to detect transfection efficiency. The transfection method of the overexpression plasmid was the same as above, all operations were performed under sterile conditions, and cells were used at fewer than six passages to ensure the reliability of the experimental results. The detailed sequences are presented in the supplementary Table 1.

Quantitative real-time polymerase chain reaction assay

Total RNA was extracted via TRIzol (Invitrogen) following the manufacturer's protocol, and the RNA concentration and purity were measured by a NanoDrop 2000 spectrophotometer (Thermo, USA). Then, 1 µg of total RNA was reversed to cDNA. The qRT-PCR reaction was performed in a 10 µl system consisting of 5 µl of 2x SYBR Green PCR Master Mix (Seven, China), 0.5 µl of 10 µM forward primer, 0.5 µl of 10 µM reverse primer, 1 µl of cDNA template, and 3 µl of nuclease-free water. The relative gene expression was calculated using the $2^{-\Delta\Delta Ct}$ method. U6 and GAPDH were used as the reference genes.

Transwell assay

For the invasion assays, the bottom of the upper chamber was coated with Matrigel (Corning, USA). Transfected cells were washed twice with PBS, and seeded into the upper chamber with the serum-free medium. The lower chamber was filled with complete medium, which served as the chemoattractant. The chambers were then incubated at 37 °C with 5% CO_2 for 48 h. After incubation, non-invading cells on the upper side of the membrane were carefully removed, and the cells that had traversed the membrane were fixed with 4% paraformaldehyde (Beyotime, China) and stained with crystal violet (Beyotime) for 15 min. The migration assay followed a similar protocol but without Matrigel coating on the bottom of chambers. Finally, the chambers were imaged under a microscope (Olympus, Japan), and

the number of invasive cells on the bottom surface of each chamber was determined using ImageJ software.

Cell proliferation assay

To assess the proliferative capacity of tumor cells, EdU incorporation and colony formation assays were performed. For EdU assay, cells were seeded into 24-well plates and incubated with EdU working solution (Invitrogen) at 37 °C for 2 h. After incubation, the cells were washed with PBS, fixed, permeabilized, and then incubated with the reaction mixture at room temperature in the dark for 30 min. Nuclei were stained with Hoechst. EdU-labeled cells were observed and imaged using a fluorescence microscope, and the percentage of EdU-positive cells in each sample was quantified using ImageJ software. For the colony formation assay, cells were digested into a single-cell suspension and seeded into 6-well plates. Tumor cells were cultured at 37 °C in a 5% CO_2 incubator until visible colonies formed. Cells were then washed with PBS, fixed, and stained. Images were captured, and colonies with a diameter greater than 1 mm were counted.

CCK-8 assay

The CCK-8 assay was used to assess the drug sensitivity of RKO and LoVo cells to 5-FU (MCE, China). Tumor cells were reseeded in 96-well plates and incubated with 100 µl of complete medium for 24 h. Subsequently, 100 µl of 5-FU solutions at varying concentrations were added to each well, with three replicate wells for each concentration. After 48 h of drug treatment, 10 µl of CCK-8 reagent (Beyotime) was added to each well and incubated at 37 °C for 1 h according to the manufacturer's instructions, and the absorbance values were determined at 450 nm using microplate reader. 5-FU concentration vs. tumor cells viability were visualized using GraphPad Prism 9.0 (GraphPad Software, USA) and the half-inhibitory concentration (IC50) was calculated.

Western blot analysis

Total proteins from tumor cells were extracted and diluted with RIPA buffer to ensure equal protein concentrations across all samples. The proteins were then separated by vertical electrophoresis using a 10% SDS-PAGE (Epizyme, China), followed by transfer onto PVDF membranes (Millipore, USA). The membranes were blocked with QuickBlock (Servicebio, China) for 10 min, and subsequently incubated overnight at 4 °C with specific primary antibodies. The following day, the membranes were incubated with HRP-conjugated secondary antibodies for 1 h at room temperature. Signal detection was performed using a chemiluminescent substrate (Beyotime), and images were captured via a Bio-Rad imaging system.

Animals

To explore the in vivo effects of CRNDE, tumor xenografts were established in 6-week-old female BALB/c nude mice obtained from Vital River (China). Tumor cells were administered to mice via subcutaneous injection. On day 25, surgical excision of the xenograft tumors was performed, during which tumor weights and volumes were measured. All the animals were kept in a specific pathogen-free environment. No unexpected mortality occurred among the mice during the experiment. The protocols were pre-approved and conducted under the policies of the Ethics Committee of Harbin Medical University Cancer Hospital.

Flow cytometry assay

Apoptosis was assessed via Annexin V-FITC Apoptosis Detection Kit (Beyotime). The cells were incubated with 5 µl Annexin V and 10 µl PI at room temperature in the dark for 15 min. The fluorescence of Annexin V and PI was then analyzed by flow cytometry, allowing for the distinction between early apoptotic cells and late apoptotic or necrotic cells. The data were analyzed using FlowJo software, and apoptosis rates were compared before and after transfection to evaluate the impact of gene silencing and overexpression.

Immunofluorescence assay

Tumor cells were seeded into 12-well plates and incubated for 24 h. The cells were then treated with 5-FU for 48 h. Following treatment, the cells were fixed with 4% paraformaldehyde for 30 min and washed three times with PBS. Permeabilization was achieved by treating the cells with 0.1% Triton X-100 for 15 min. After additional washes with PBS, the cells were blocked with 5% BSA at 37 °C for 2 h. Immunostaining was performed using a primary antibody against GSDMD, followed by incubation with a corresponding fluorescence-conjugated secondary antibody at 37 °C in the dark for 1 h. Nuclei were stained with DAPI. After washing, images were captured using a fluorescence microscope. The fluorescence intensity was analyzed and compared with that of control groups to assess pyroptosis in tumor cells.

RNA pull-down assay

The RNA pull-down assay was employed to investigate the direct interaction between CRNDE RNA and RIPK3 protein. Cells were then lysed and the lysates were subjected

to ultracentrifugation to remove cell debris. Biotin-labeled CRNDE RNA probes were incubated with the cell lysates, allowing the formation of RNA-protein complexes. Magnetic beads were then added to capture the RNA-protein complexes, followed by magnetic separation and extensive washing to eliminate non-specific binding. The complexes were eluted using SDS-PAGE, and the interaction between CRNDE and RIPK3 was confirmed and quantified via Western blot analysis using RIPK3-specific antibodies. The antisense RNA probe was used as the negative control to ensure the specificity of the interaction.

Fluorescence in situ hybridization assay

To determine the subcellular localization of CRNDE and RIPK3, FISH was performed. CC cells were first fixed with 4% paraformaldehyde for 15 min and permeabilized with 0.5% Triton X-100 for 10 min. Then, cells were respectively hybridized with the probes for CRNDE, followed by counterstaining with DAPI, according to the manufacturer's protocols (Ribobio, China). Moreover, the cellular localization of RIPK3 in tumor cells was detected by IF. A confocal laser scanning microscope (Zeiss, Germany) was utilized to observe the relative positions of probes in tumor cells.

Co-immunoprecipitation assay

Tumor cells were meticulously washed with ice-cold PBS and lysed with Non-Denaturing Lysis Buffer (Abbkine, China). The resulting lysates were subjected to centrifugation for debris removal. Immunoprecipitation was subsequently conducted by incubating the pre-cleared lysates with Protein A/G Magnetic Beads (Abbkine) coated with RIPK3 primary antibody, and the incubation was carried out overnight at 4 °C. After the binding process, the bead-protein complexes were subjected to thorough washing to eliminate any unbound proteins and contaminants, utilizing Wash Buffer (Abbkine). Elution of the immunoprecipitated protein complexes was achieved by adding SDS-PAGE Loading Buffer (Seven). Subsequent Western blot analysis was employed to discern the interacting partners of RIPK3.

Chromatin immunoprecipitation assay

The tumor cells were resuspended in PBS containing 1% formaldehyde and cross-linked at 37 °C for 10 min, followed by washing with PBS containing 1 mM PMSF and quenching with 1.375 M glycine and centrifugation to collect the cells. For nuclear preparation, cells were lysed using Lysis Buffer (BersinBio, China), and chromatin was sheared by sonication to fragments of 200–800 bp. The supernatant was collected, and DNA fragment size was assessed by agarose gel electrophoresis. Samples were then divided into IP, IgG, and input groups, with antibodies added for incubation at 4 °C for 12–16 h. Immunoprecipitation was performed using Protein A/G magnetic beads. Following elution, decrosslinking, and precipitation, enriched DNA was obtained, and the enrichment efficiency was validated by qRT-PCR.

Luciferase reporter assay

To assess the impact of TFAP2A on CRNDE promoter activity, a luciferase reporter assay was conducted. Cells were cultured to 60–70% confluence, and transfection mixtures were prepared. Wild- and mutant-type luciferase reporter plasmids were separately transfected into the cells, followed by incubation at 37 °C for 24 h. After incubation, cells were collected, washed with ice-cold PBS, and lysed according to the instructions of the luciferase assay kit to obtain cell lysates. The cell lysates were then added to a 96-well plate along with the luciferase substrate, and luciferase activity was immediately measured using a microplate reader.

Statistics

Statistical analysis was conducted using SPSS software (IBM SPSS, USA). For data conforming to the Gaussian distribution, independent samples *t*-test or *ANOVA* was applied, whereas for non-normally distributed data, the *Mann-Whitney U* test or *Kruskal-Wallis* test was used. Graphical representations were generated using GraphPad Prism 9.0 (USA) to visually portray data distribution and research outcomes. Results are presented as mean ± standard deviation, and p-value less than 0.05 were considered statistically significant.

Results

CRNDE is abnormally overexpressed in CC

In order to find out the lncRNAs that may regulate the development of CC, we downloaded the RNA-seq data from TCGA and GEO databases (TCGA-COAD, GSE84983, GSE110715, GSE117830, GSE146009, and GSE180440), analyzed the expression differences with the help of R language and intersected the differential genes ($|\log2\text{fold-change}|=1.5$, $p<0.05$). Finally, we selected CRNDE, which was the most significantly expressed gene in CC patients, as the research object (Fig. 1A-C). Subsequently, qRT-PCR quantitative analysis of common colon cell lines revealed that CRNDE expression was significantly upregulated in tumor cells, consistent with the results of bioinformatics

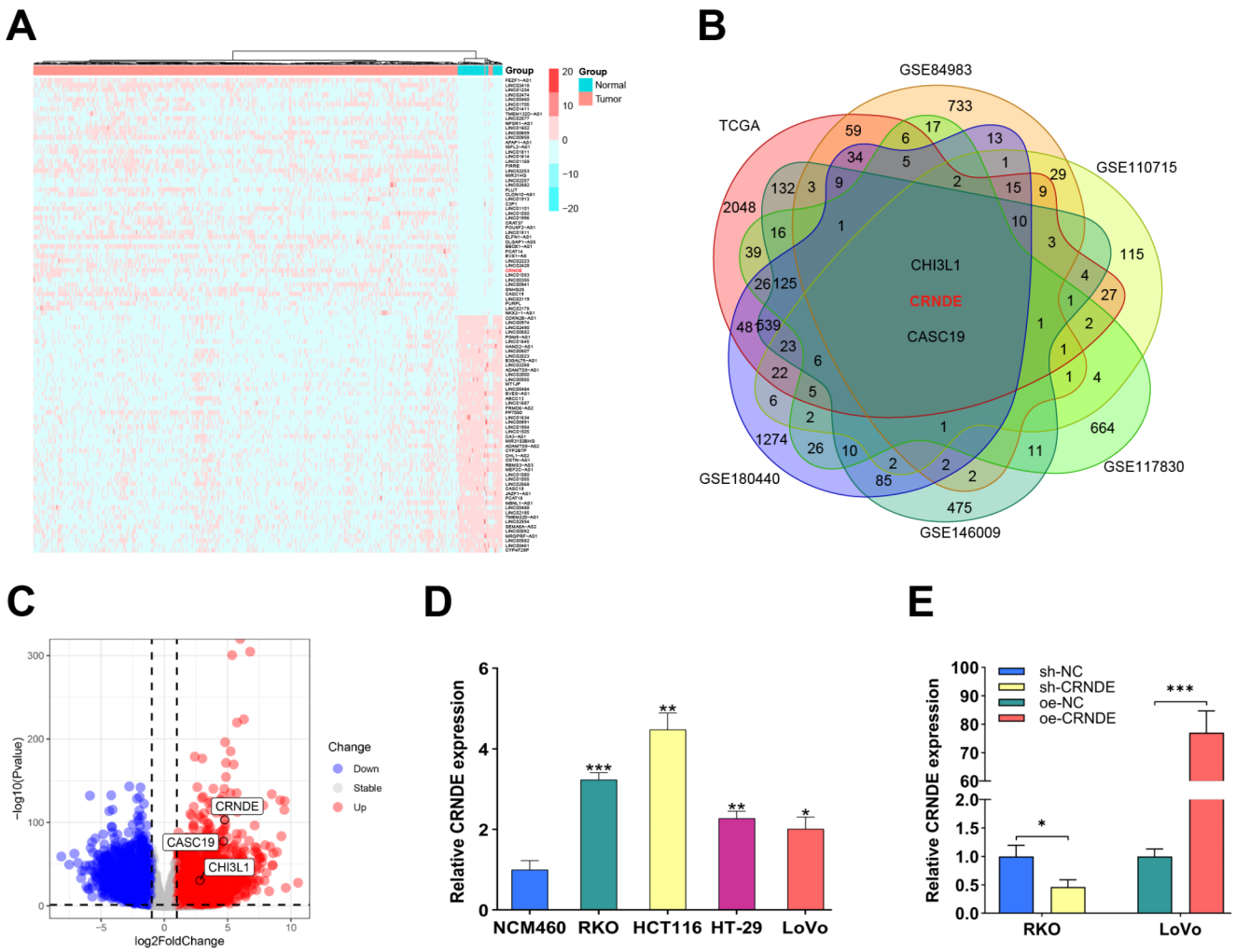

Fig. 1 Expression analysis and validation of CC-related lncRNAs. (**A-C**) Differentially expressed genes in CC (TCGA-COAD, GSE84983, GSE110715, GSE117830, GSE146009, GSE180440) were analyzed using R language (|log2 fold change| = 1.5, $p<0.05$) and intersected. (**D**) Expression levels of CRNDE in common CC and normal cell lines. (**E**) Validation of plasmid transfection efficiency via qRT-PCR. $^{*}p<0.05$, $^{**}p<0.01$, $^{***}p<0.001$

analysis. The RKO cell with the most significant CRNDE expression and the LoVo cell with relatively lower expression were selected for further research. (Fig. 1D).

CRNDE modulates CC progression both *in vitro* and *in vivo*

First, we manually regulated the expression of CRNDE in RKO and LoVo cells to explore the biological functions of CRNDE in CC. As shown in Fig. 1E, transfection of specific shRNA significantly inhibited the expression of CRNDE in RKO cells, whereas the transfection of the CRNDE plasmid markedly upregulated CRNDE expression in LoVo cells. The results of clone formation and EdU assays indicated that the number of cell colonies and the proportion of EdU-positive cells were significantly reduced after the exogenous downregulation of CRNDE in RKO cells, while the overexpression of CRNDE significantly increased the cell proliferation ability (Fig. 2A-B). The results of Transwell assay showed that silencing CRNDE significantly repressed the migration and invasion of RKO cells, while the CRNDE overexpression promoted the migration and invasion of LoVo cells (Fig. 2C-D). Since epithelial-mesenchymal transition (EMT) is the critical step in tumor cell migration and invasion, we further explored the potential role of CRNDE in regulating EMT in tumor cells. Western blot analysis showed that the expression of E-cadherin was significantly up-regulated, while the expression of N-cadherin and Vimentin was downregulated after inhibition of CRNDE expression. Conversely, CRNDE overexpression promoted N-cadherin and Vimentin expression in LoVo cells, thereby facilitating EMT progression in tumor cells (Fig. 3A, Fig. S1A). Given that 5-FU is the cornerstone of chemotherapy for CC, we measured the IC50 of 5-FU in

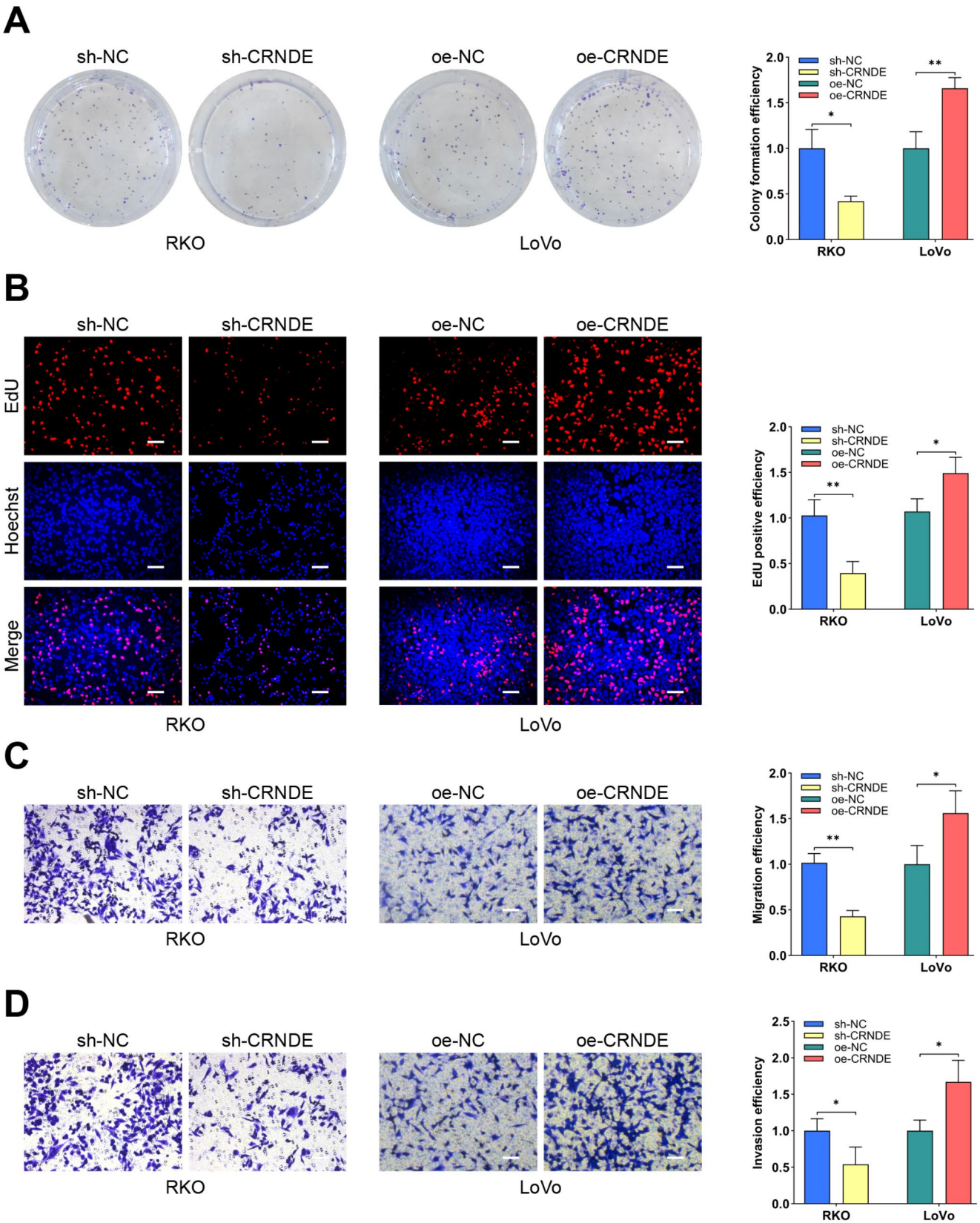

Fig. 2 Effects of CRNDE on tumor cell proliferation and invasion. (**A-B**) Assessment of tumor cell proliferation using colony formation and EdU assays. (**C-D**) Evaluation of migration and invasion capabilities of RKO and LoVo cells through Transwell assays. $^{*}p<0.05$, $^{**}p<0.01$

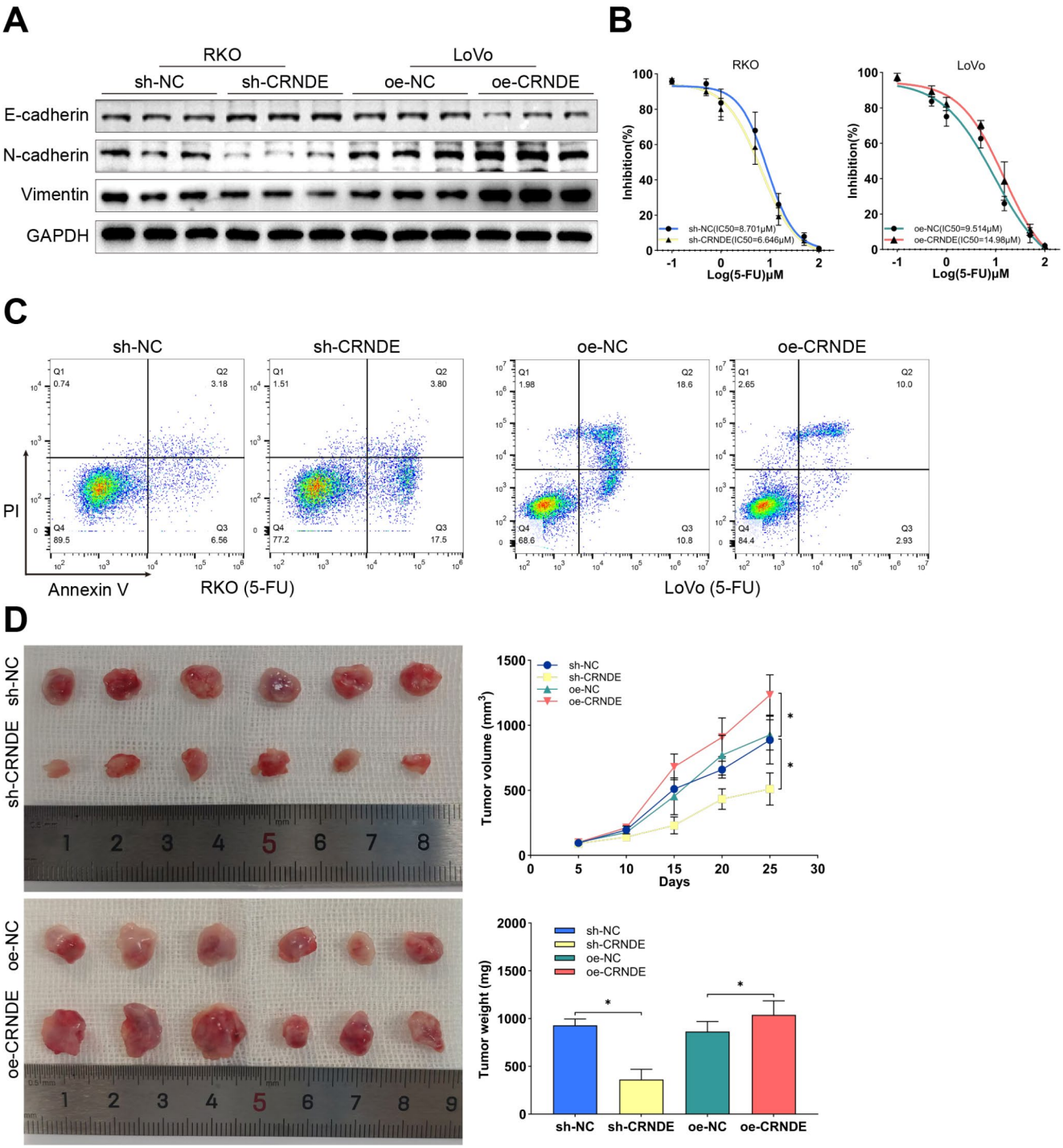

Fig. 3 CRNDE modulates CC malignancy behaviors in vitro and in vivo. (**A**) Western blot analysis highlighting changes in the expression of epithelial-mesenchymal transition (EMT) markers. (**B**) CCK-8 assay assessing the sensitivity of RKO and LoVo cells to 5-FU. (**C**) Flow cytometry assay evaluating apoptosis changes in 5-FU treated tumor cells. (**D**) Measurement of weight and volume of subcutaneous tumors following CRNDE regulation. $^{*}p<0.05$

RKO and LoVo cells, and selected the appropriate concentration of 5-FU to explore the regulatory effect of CRNDE on the drug sensitivity of these cells. Subsequent CCK-8 and flow cytometry assays results showed that transfection of specific shRNA enhanced the sensitivity of RKO cells to 5-FU, whereas the overexpression of CRNDE decreased the sensitivity of LoVo cells to 5-FU (Fig. 3B-C). To investigate the effects of CRNDE in vivo, xenograft tumor models were established. CRNDE knockdown significantly reduced

tumor volume and weight, while CRNDE overexpression promoted xenograft growth (Fig. 3D).

CRNDE promotes 5-FU resistance by inhibiting pyroptosis via RIPK3 downregulation

To further elucidate the mechanism by which CRNDE regulates CC, we stratified the patients into high- and low-expression groups according to the median FPKM level of CRNDE. The results of subsequent GSEA analysis revealed that the function of the NOD-like pathway (pyroptosis-related signaling pathway) was inhibited in high-expression group (Fig. 4A). Recent studies have shown that pyroptosis plays important roles in the initiation, development, and treatment of tumors (Fang et al. 2023; Feng et al. 2023; Peng et al. 2022; Tan et al. 2022; Zhang et al. 2022). Based on the aforementioned bioinformatics analysis results, we hypothesized that CRNDE might promote cancer by inhibiting the pyroptosis process in tumor cells. On the basis of this hypothesis, we conducted an in-depth study on the genes enriched by the NOD-like pathway and finally selected RIPK3 as the focus of subsequent research basis

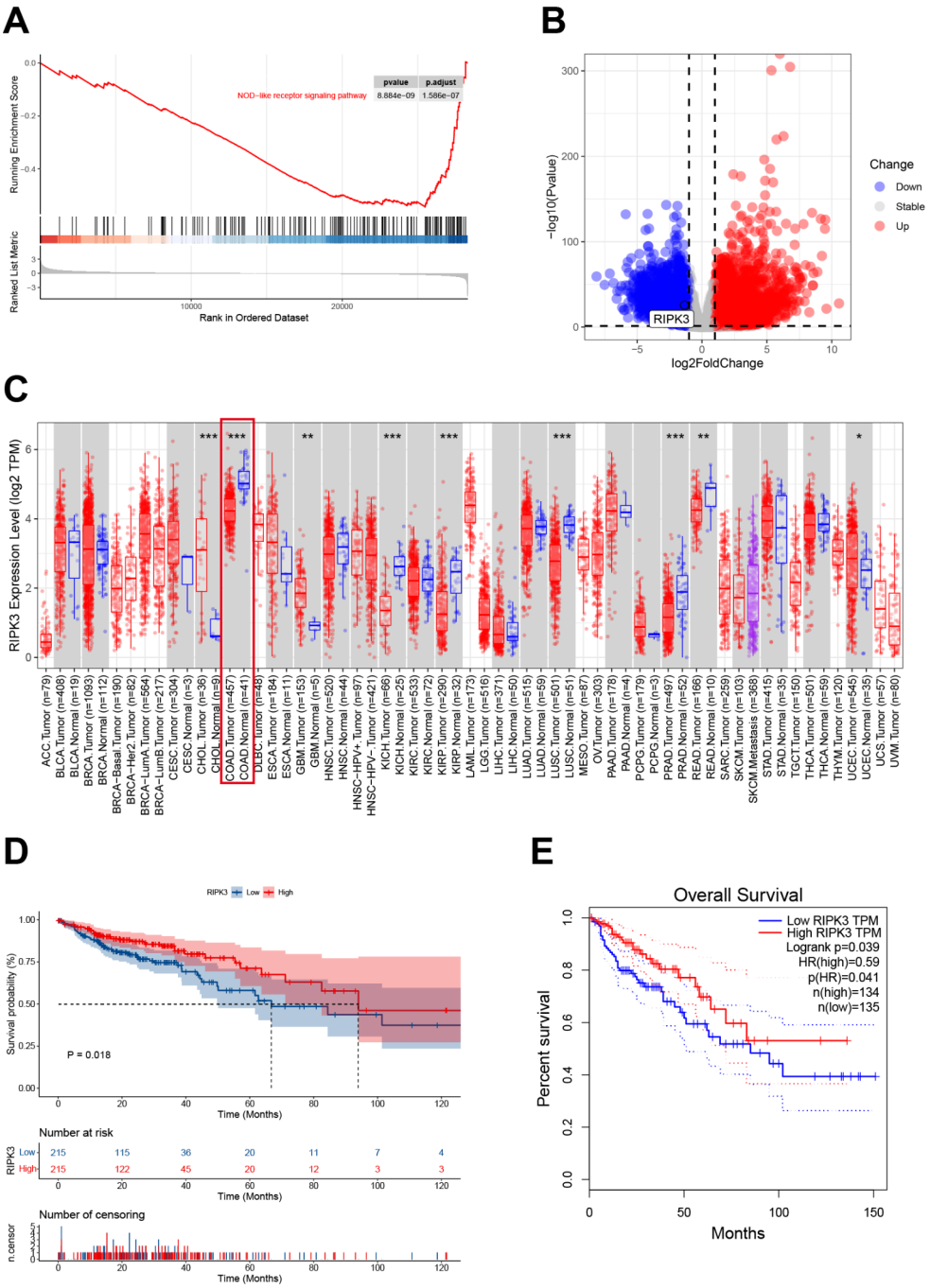

Fig. 4 RIPK3 is the downstream target gene of CRNDE. (**A**) GSEA analysis identifies dysregulated pathways in CC. (**B**) Selection of differentially expressed genes within the identified pathways. (**C**) Expression profile of RIPK3 across various cancer types. (**D-E**) Impact of RIPK3 expression levels on the survival of CC patients

on prior knowledge and the results of differential analysis and survival analysis (Fig. 4B-E). We subsequently carried out in vitro experiments to verify the prediction results, and the Western blotting results showed that RIPK3 was downregulated in tumor cells (Fig. S1B). In addition, silencing CRNDE upregulated the expression level of RIPK3, while transfection of CRNDE overexpression plasmid inhibited RIPK3 expression (Fig. S1C), suggesting that there was a regulatory relationship between CRNDE and RIPK3. Moreover, we observed that some tumor cells exhibited characteristic pyroptotic features in response to 5-FU treatment, such as cell swelling and cytoplasmic ballooning (Fig. 5A). Previous studies have established that RIPK3 mediates pyroptosis by activating the NLRP3 inflammasome (Lawlor et al. 2015). Interestingly, our findings revealed that the knockdown or overexpression of RIPK3 could partially restore the drug sensitivity of tumor cells that was altered by the knockdown or overexpression of CRNDE (Fig. 5A). Therefore, we further explored the effect of the CRNDE/RIPK3 axis on the pyroptosis in RKO and LoVo cells. Combined with the results of flow cytometry, immunofluorescence, Western blot and corresponding rescue assays, we confirmed that CRNDE promotes 5-FU resistance by suppressing pyroptosis via the modulation of RIPK3 expression (Fig. 5B-D).

CRNDE promotes ubiquitin-mediated RIPK3 degradation via K63-linked ubiquitination

Next, we conducted an in-depth study on the intrinsic mechanism of CRNDE regulates RIPK3 expression. Initially, we considered the classical competing endogenous RNA (ceRNA) mechanism, however, the RNA-seq results showed that there was no significant correlation between RIPK3 and CRNDE expression at the RNA level (Fig. S1D-F). Through literature search, we learned that (1) some lncRNAs can directly bind to and regulate protein expression and that (2) RIPK3 degradation relies on ubiquitination modifications (Cai et al. 2022; Onizawa et al. 2015; Wang et al. 2023). Therefore, we hypothesized that CRNDE may regulate its expression by directly binding to RIPK3 and promoting its ubiquitinated degradation. To test this hypothesis, we designed the corresponding experiments. The results of FISH assay showed that CRNDE and RIPK3 co-localized in the cytoplasm of colon cancer cells (Fig. 6A). The results of RNA-pull down assay confirmed that RIPK3 could be precipitated by CRNDE RNA, or antisense CRNDE RNA (Fig. 6B), suggesting that CRNDE RNA could directly bind to RIPK3. Western blot analysis showed that RIPK3 expression decreased over time after treatment with Cycloheximide (CHX, a protein synthesis inhibitor), and the decay rate of RIPK3 in the oe-CRNDE group increased significantly, while the attenuation degree in the sh-CRNDE group was significantly lower compare to sh-NC group (Fig. 6C, Fig. S1G). In addition, treatment with MG132 or Lactacystin (the proteasome inhibitor) inhibited the attenuation of RIPK3 protein, while treatment with the lysosomal inhibitor Chloroquine or negative control DMSO showed no significant change (Fig. 6D, Fig. S2A), suggesting that RIPK3 protein is degraded through the proteasome pathway. Further Co-IP experiments confirmed that CRNDE promoted the ubiquitination of RIPK3 (Fig. 6E). Subsequently, in vitro ubiquitination experiments were performed to explore the types of ubiquitin linkages on RIPK3, and ubiquitin (Ub) vectors with the single lysine mutations were co-transfected with RIPK3. Western blot results showed that there were multiple forms of ubiquitin linkages in RIPK3 (Fig. 6F). Interestingly, overexpression of CRNDE selectively promoted ubiquitination of the Ub-K63 type, but had having no effect on other forms (Fig. 6G, S2B-G).

TFAP2A functions as the upstream regulator of CRNDE

Finally, we delved into the upstream regulatory mechanism of CRNDE. By utilizing the UCSC (http://genome-asia.ucsc.edu/) database, we found that TFAP2A may be the potential promoter of CRNDE (score = 431, $p < 10^{-4}$). The JASPAR database (http://JASPAR.genereg.net/) shows the presence of a TFAP2A binding site (relative score > 0.98) in the upstream region of CRNDE (Fig. 7A). In addition, bioinformatics analysis results showed that TFAP2A was abnormally upregulated in various malignant tumors and served as oncogene (Fig. 7B). In addition, we observed that TFAP2A was abnormally overexpressed in tumor cells (Fig. S2H). Luciferase reporter assays also confirmed that TFAP2A was able to activate the expression of wild-type luciferase plasmids, but not mutants (Fig. 7C-D). The results of the ChIP assay further support the relationship between TFAP2A and the upstream regulation of CRNDE (Fig. 7E). Alphafold3 model also indicated that TFAP2A bond to the CRNDE promoter region (Fig. 7F). The above experimental results show that TFAP2A functions as an upstream regulator of CRNDE, which induces high-level expression of CRNDE by binding to its promoter region.

Discussion

The incidence of CC is increasing annually and trending younger (Qu et al. 2022; Wong et al. 2023). Despite recent advances in targeted therapies and immunotherapies, surgery, chemotherapy, and radiotherapy remain the standard

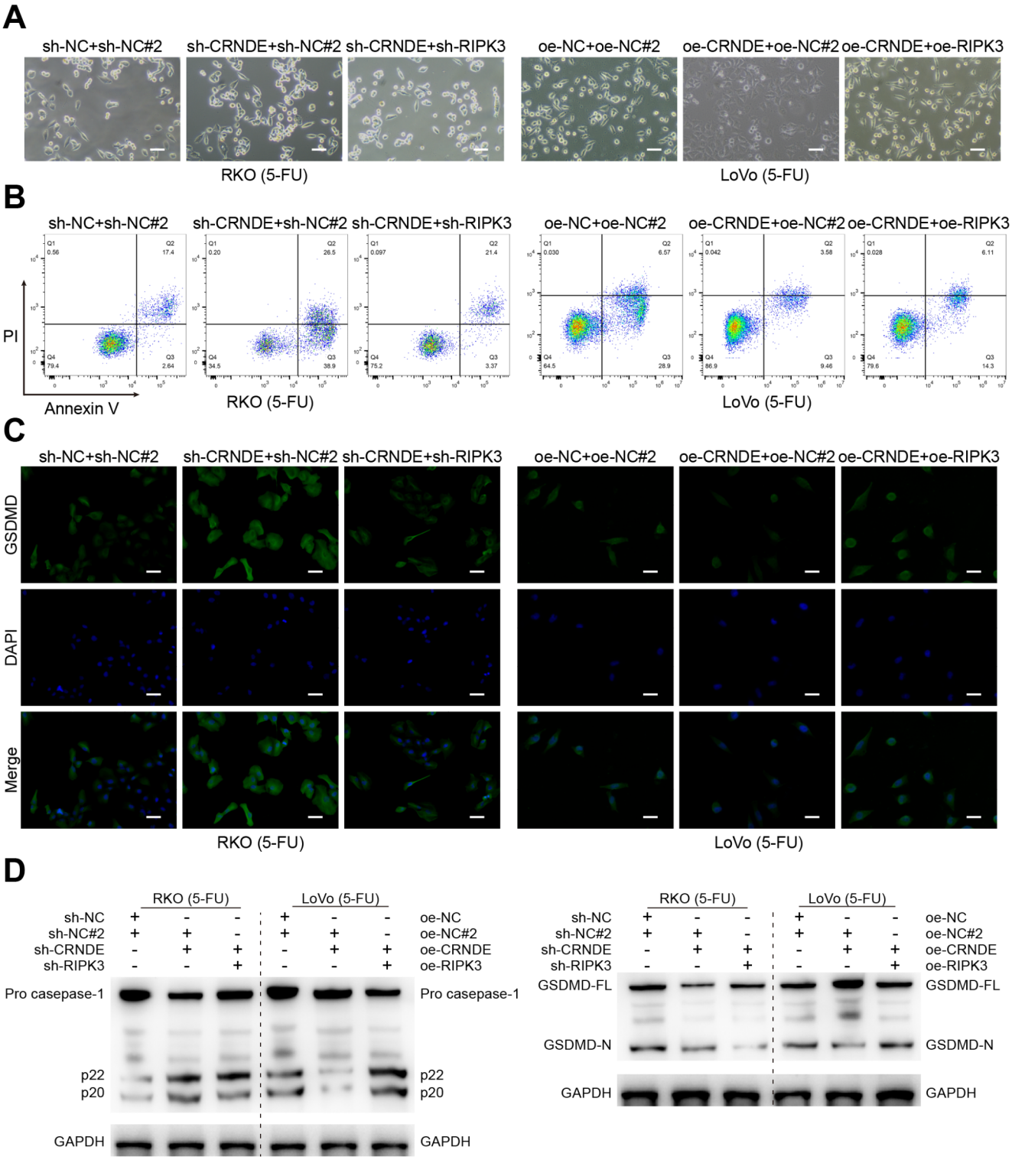

Fig. 5 CRNDE influences the pyroptosis process in tumor cells by regulating RIPK3 expression. (**A**) Morphological changes in tumor cells after 5-FU treatment observed under a light microscope. (**B**) Flow cytometry analysis of RIPK3 expression's effect on 5-FU-induced pyroptosis in tumor cells. (**C**) Immunofluorescence showing the influence of RIPK3 levels on pyroptosis in cells treated with 5-FU. (**D**) Western blot demonstrating changes in pyroptosis marker proteins across different treatment groups

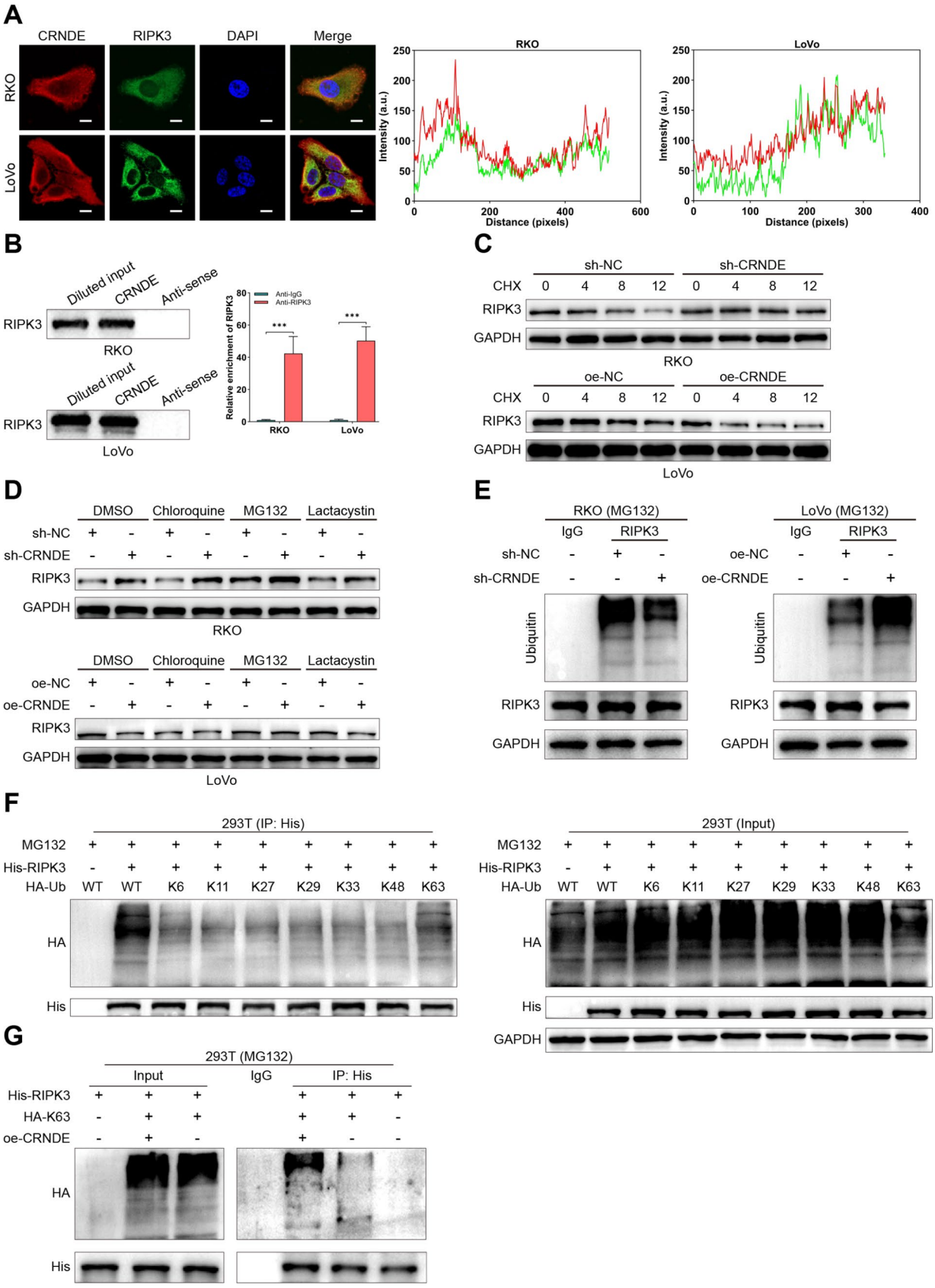
A
CRNDE
RIPK3
DAPI
Merge
RKO
LoVo
RKO
LoVo
Intensity (a.u.)
Distance (pixels)
B
Diluted input
CRNDE
Anti-sense
RIPK3
RKO
LoVo
Anti-IgG
Anti-RIPK3
Relative enrichment of RIPK3
C
sh-NC
sh-CRNDE
CHX
0
4
8
12
RIPK3
GAPDH
RKO
oe-NC
oe-CRNDE
LoVo
D
DMSO
Chloroquine
MG132
Lactacystin
sh-NC
sh-CRNDE
oe-NC
oe-CRNDE
RIPK3
GAPDH
RKO
LoVo
E
RKO (MG132)
LoVo (MG132)
IgG
RIPK3
Ubiquitin
F
293T (IP: His)
293T (Input)
MG132
His-RIPK3
HA-Ub
WT
K6
K11
K27
K29
K33
K48
K63
HA
His
GAPDH
G
293T (MG132)
Input
IgG
IP: His
His-RIPK3
HA-K63
oe-CRNDE
HA
His

Fig. 6 CRNDE targets RIPK3 to promote its ubiquitin-mediated degradation. (**A**) Localization of CRNDE and RIPK3 in RKO and LoVo cells as visualized by FISH assay. (**B**) RNA-pulldown assay demonstrating the interaction between CRNDE and RIPK3. (**C**) Western blot analysis showing the effect of CRNDE expression levels on the degradation rate of RIPK3. (**D**) Impact of proteasome inhibitors (MG132 and Lactacystin) and autophagolysosome inhibitor (Chloroquine) on RIPK3 expression levels. (**E**) Effect of CRNDE expression on the ubiquitination levels of RIPK3. (**F**) Co-IP assays investigating the ubiquitination forms of RIPK3. (**G**) Co-IP assays examining the effect of CRNDE on K63-linked ubiquitination of RIPK3

treatments for CC. Therefore, exploration of the internal mechanism of the occurrence and development of CC is urgently needed to provide new ideas and directions for its clinical treatment.

Long non-coding RNAs have long been considered "cold spots" in genomic transcripts. With the deepening of genomics research, lncRNAs have gradually been recognized as important regulators of biological processes, participating in the regulation of gene expression at different levels such

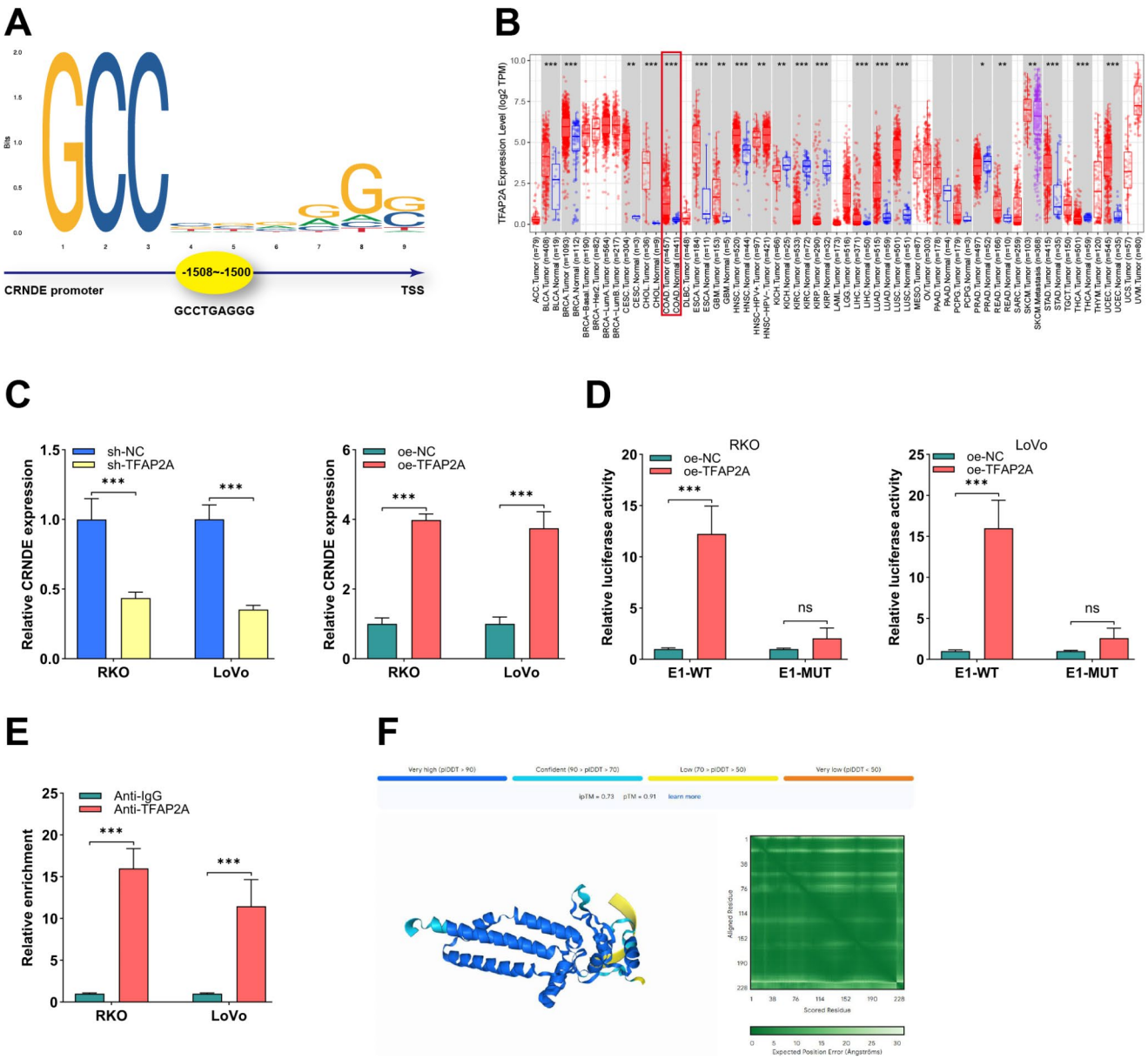

Fig. 7 TFAP2A is the upstream transcription factor of CRNDE. (**A**) Schematic illustration of the interaction between TFAP2A and CRNDE. (**B**) Expression profile of TFAP2A across various cancer types. (**C**) qRT-PCR validation of TFAP2A regulatory effect on CRNDE. (**D**) Luciferase reporter assay confirming the interaction between TFAP2A and CRNDE. (**E**) ChIP assay verifying the binding relationship between TFAP2A and CRNDE. (**F**) AlphaFold3 model predicting the interaction between TFAP2A and CRNDE. *** $p<0.001$

as chromatin remodeling, transcription and post-transcription, and influencing key cellular processes such as proliferation, differentiation, apoptosis, migration and metabolism (Elimam et al. 2024). In this context, research on lncRNAs offers new breakthroughs and directions for understanding CC. Recent studies have identified that CRNDE functions as an oncogene in multiple malignancies, and regulates biological behaviors such as tumor autophagy and drug resistance through the ceRNA mechanism, making it a bright star in cancer research.

First, we analyzed the RNA-seq data of CC patients by R language, and selected CRNDE, which was abnormally high in CC tumor tissues, as the research object of this study. In addition, we performed RT-qPCR analysis of CC cell lines to verify the accuracy of the bio-informatics analysis results, confirming that CRNDE was abnormally high in CC. Next, we conducted clone formation, Transwell, EdU, CCK-8, flow cytometry, Western blot experiments and established xenograft models to explore the biological function of CRNDE in CC, and the results showed that CRNDE promoted the development of CC in vitro and in vivo. To further elucidate the mechanism of CRNDE in regulating CC, we grouped RNA-seq data according to the average expression of CRNDE, and performed GSEA enrichment analysis, and the results showed that NOD-like pathway function was inhibited in the high-expression CRNDE group. Through reviewing a large number of literatures, we learned that RIPK3, as the star protein of the NOD-like pathway, can inhibit the development of tumors by promoting the pyroptosis in tumor cells. The results of the TimeR2.0 (http://timer.cistrome.org/) and GEPIA (http://gepia.cancer-pku.cn/) website showed that RIPK3 was expressed at low level in CC tumor tissues and was closely related to the prognosis of CC patients. In addition, in vitro experiments showed that the expression level of RIPK3 protein was closely related to the expression of CRNDE, and rescue experiments confirmed that CRNDE exerted a pro-cancer effect by regulating the expression of RIPK3. Further mechanistic studies showed that there was no significant correlation between the expression level of RIPK3 mRNA and the expression of CRNDE. Combined with the literature, we boldly hypothesized that CRNDE regulated the expression of RIPK3 by directly binding to it and inhibiting its ubiquitination degradation. The fluorescence colocalization results confirmed that CRNDE and RIPK3 co-localized in the cytoplasm of tumor cells, laying the foundation for the interaction between the two. RNA pull-down experiments confirmed that CRNDE could directly bind to RIPK3. In addition, Western blot assay results confirmed that RIPK3 was degraded by the ubiquitination pathway in tumor cells and was regulated by CRNDE. The results of Co-IP experiments revealed that CRNDE selectively promoted the ubiquitination of the Ub-K63 type. These results confirm our hypothesis and clarify the mechanism by which CRNDE regulates the expression of RIPK3 by directly binding to RIPK3 and promoting its ubiquitination degradation. Finally, we look at the upstream regulatory mechanisms of CRNDE. The literature survey results showed that TFAP2A was abnormally expressed in many malignant tumors and played pivotal roles in cancer progression. Western blot results showed that TFAP2A was abnormally high in CC cells, and its expression level was closely related to CRNDE. In addition, the results of ChIP and luciferase reporter experiments and model predictions also confirmed that TFAP2A passed the junction with the E1 site of CRNDE.

In this study, we primarily employed in vitro cell models and animal experimental models to investigate the effects of CRNDE on tumor behavior. However, the use of these models has certain limitations. For instance, in vitro assays cannot fully replicate the complex tumor microenvironment in vivo, and animal models differ from human tumors in terms of genetic background and immune system characteristics. These discrepancies may influence the interpretation of CRNDE's actual mechanisms in tumor behavior. Future studies should consider utilizing more clinically relevant models, such as patient-derived organoids or humanized animal models, to further validate the functions of CRNDE. Additionally, to clarify the potential of CRNDE as a therapeutic target, we plan to design more specific hypotheses and experiments. For example, future research could explore the molecular mechanisms by which CRNDE regulates downstream signaling pathways, leverage nanocarrier drug delivery systems, and assess the relationship between CRNDE expression levels and patient prognosis to evaluate its clinical therapeutic value.

At present, there has been some progress in research on lncRNAs as biomarkers, therapeutic targets, and novel epigenetic intervention tools (Sun et al. 2018; Vergara et al. 2012; Yu et al. 2015; Zhong et al. 2019), but the depth and breadth still need to be improved. In particular, in terms of elucidating the mechanism of action of lncRNA, existing studies have not yet fully revealed their specific functions and regulatory networks. Technical challenges further limit the clinical application prospects of lncRNAs. However, in the face of these challenges, we will never stop at its laurels. With the continuous innovation of technology and the deepening of scientific research, we have reason to believe that the targeted therapy technology based on lncRNA will gradually mature, and its clinical application is just around the corner.

Conclusion

In summary, we reported for the first time that CRNDE promotes the development of CC as oncogene, and elucidated the TFAP2A/CRNDE/RIPK3 axis, which opened up a new situation in the research of colon cancer.

Supplementary Information The online version contains supplementary material available at https://doi.org/10.1007/s10142-025-01545-w.

Author contributions All authors made a significant contribution to the work reported. X.G., Y.H., T.W., J.X., F.I. and L.Y. designed the study; X.G., Y.H., H.L. and L.W. prepared samples and generated the experiments; X.G. collected and organized data and wrote the manuscript. G.M., Y.H., H.X., H.W., S.L. and P.H. provided suggestions and revised the paper. All authors have read and agreed to the published version of the manuscript.

Funding This research was funded by the National Natural Science Foundation of China (82072640), Climbing program of Harbin Medical University Cancer Hospital (PDYS-2024-14), The Collaborative Innovation Cultivation Project of Higher Education Institutions in Heilongjiang Province (LJGXCG2023-087).

Data availability The datasets generated during the current study are available from the corresponding author on reasonable request.

Declarations

Competing interests The authors declare no competing interests.

References

Babcook MA, Sramkoski RM, Fujioka H et al (2014) Combination simvastatin and metformin induces G1-phase cell cycle arrest and Ripk1- and Ripk3-dependent necrosis in C4-2B osseous metastatic castration-resistant prostate cancer cells. Cell Death Dis. 2014, 5(11): e1536. https://doi.org/10.1038/cddis.2014.500

Brenner H, Hoffmeister M (2021) Striving to optimize colorectal cancer prevention. Nat Rev Gastroenterol Hepatol. 2021, 18(10): 677–678. https://doi.org/10.1038/s41575-021-00494-6

Cai Z, He X, Liu S et al (2022) Linear ubiquitination modification of NR6A1 by LUBAC inhibits RIPK3 kinase activity and attenuates apoptosis of vascular smooth muscle cells. J Biochem Mol Toxicol. 2022, 36(8): e23091. https://doi.org/10.1002/jbt.23091

Chen Z, Yu C, Zhan L et al (2016) LncRNA CRNDE promotes hepatic carcinoma cell proliferation, migration and invasion by suppressing miR-384. Am J Cancer Res. 2016, 6(10): 2299–2309. Retrieved from https://www.ncbi.nlm.nih.gov/pubmed/27822419

Chen B, Dragomir MP, Yang C et al (2022) Targeting non-coding RNAs to overcome cancer therapy resistance. Signal Transduct Target Ther. 2022, 7(1): 121. https://doi.org/10.1038/s41392-022-00975-3

Chen J, Gao Y, Zhong J et al (2024) Lnc-H19-derived protein shapes the immunosuppressive microenvironment of glioblastoma. Cell reports. Medicine. 2024, 5(11): 101806. https://doi.org/10.1016/j.xcrm.2024.101806

Cho E, Lee JK, Park E et al (2018) Antitumor activity of HPA3P through RIPK3-dependent regulated necrotic cell death in colon cancer. Oncotarget. 2018, 9(8): 7902–7917. https://doi.org/10.18632/oncotarget.24083

Conev NV, Dimitrova EG, Bogdanova MK et al (2019) RIPK3 expression as a potential predictive and prognostic marker in metastatic colon cancer. Clin Invest Med. 2019, 42(1): E31-E38. https://doi.org/10.25011/cim.v42i1.32390

Ding X, Zhang Y, Liang J et al (2022) The long non-coding RNA CRNDE promotes osteosarcoma proliferation and migration by sponging miR-136-5p/MRP9 axis. Ann Transl Med. 2022, 10(15): 835. https://doi.org/10.21037/atm-22-3602

Duangthim N, Lomphithak T, Saito-Koyama R et al (2024) Prognostic significance and response to immune checkpoint inhibitors of RIPK3, MLKL and necroptosis in non-small cell lung cancer. Sci Rep. 2024, 14(1): 21625. https://doi.org/10.1038/s41598-024-72545-2

Elimam H, Moussa R, Radwan AF et al (2024) LncRNAs orchestration of gastric cancer - particular emphasis on the etiology, diagnosis, and treatment resistance. Funct Integr Genomics. 2024, 24(5): 175. https://doi.org/10.1007/s10142-024-01450-8

Fang X, Chen Z, Zhou W et al (2023) Boosting Glioblastoma Therapy with Targeted Pyroptosis Induction. Small. 2023, 19(30): e2207604. https://doi.org/10.1002/smll.202207604

Feng WQ, Zhang YC, Xu ZQ et al (2023) IL-17A-mediated mitochondrial dysfunction induces pyroptosis in colorectal cancer cells and promotes CD8+T-cell tumour infiltration. J Transl Med. 2023, 21(1): 335. https://doi.org/10.1186/s12967-023-04187-3

Fenocchio E (2024) Rethinking colorectal cancer prognosis: beyond microsatellite status. Lancet Gastroenterol Hepatol. 2024, 9(7): 585–586. https://doi.org/10.1016/S2468-1253(24)00129-8

Gu Y, Li C, Ren X et al (2024) Long Noncoding RNA CRNDE Promotes Gastric Cancer Progression through Targeting miR-136-5p/MIEN1. Cancer Biother Radiopharm. 2024. https://doi.org/10.1089/cbr.2023.0179

Lawlor KE, Khan N, Mildenhall A et al (2015) RIPK3 promotes cell death and NLRP3 inflammasome activation in the absence of MLKL. Nat Commun. 2015, 6: 6282. https://doi.org/10.1038/ncomms7282

Li J, Li Y, Wang D et al (2024) PLAG1 interacts with GPX4 to conquer vulnerability to sorafenib induced ferroptosis through a PVT1/miR-195-5p axis-dependent manner in hepatocellular carcinoma. Journal of experimental & clinical cancer research. 2024, 43(1): 143. https://doi.org/10.1186/s13046-024-03061-4

Liang J, Tian X, Zhou M et al (2024) Shikonin and chitosan-silver nanoparticles synergize against triple-negative breast cancer through RIPK3-triggered necroptotic immunogenic cell death. Biomaterials. 2024, 309: 122608. https://doi.org/10.1016/j.biomaterials.2024.122608

Liu K, Xiao Y, Gan L et al (2023) Structural basis for specific DNA sequence motif recognition by the TFAP2 transcription factors.

Nucleic Acids Res. 2023, 51(15): 8270–8282. https://doi.org/10.1093/nar/gkad583
Ma Y, Yang Y, Wang F et al (2016) Long non-coding RNA CCAL regulates colorectal cancer progression by activating Wnt/beta-catenin signalling pathway via suppression of activator protein 2alpha. Gut. 2016, 65(9): 1494–1504. https://doi.org/10.1136/gutjnl-2014-308392
Ma W, Song M, Chan AT (2021) Is Colorectal Cancer Screening Absolutely Beneficial for Older Adults? JAMA Oncol. 2021, 7(11): 1728–1729. https://doi.org/10.1001/jamaoncol.2021.4155
Matsui M, Corey DR (2017) Non-coding RNAs as drug targets. Nat Rev Drug Discov. 2017, 16(3): 167–179. https://doi.org/10.1038/nrd.2016.117
Onizawa M, Oshima S, Schulze-Topphoff U et al (2015) The ubiquitin-modifying enzyme A20 restricts ubiquitination of the kinase RIPK3 and protects cells from necroptosis. Nat Immunol. 2015, 16(6): 618–627. https://doi.org/10.1038/ni.3172
Peng X, Na R, Zhou W et al (2022) Nuclear translocation of Gasdermin D sensitizes colorectal cancer to chemotherapy in a pyroptosis-independent manner. Oncogene. 2022, 41(47): 5092–5106. https://doi.org/10.1038/s41388-022-02503-7
Qu R, Ma Y, Zhang Z et al (2022) Increasing burden of colorectal cancer in China. Lancet Gastroenterol Hepatol. 2022, 7(8): 700. https://doi.org/10.1016/S2468-1253(22)00156-X
Schulte JH, Kirfel J, Lim S et al (2008) Transcription factor AP2alpha (TFAP2a) regulates differentiation and proliferation of neuroblastoma cells. Cancer Lett. 2008, 271(1): 56–63. https://doi.org/10.1016/j.canlet.2008.05.039
Shao K, Shi T, Yang Y et al (2016) Highly expressed lncRNA CRNDE promotes cell proliferation through Wnt/beta-catenin signaling in renal cell carcinoma. Tumour Biol 2016. https://doi.org/10.1007/s13277-016-5440-0
Slack FJ, Chinnaiyan AM (2019) The Role of Non-coding RNAs in Oncology. Cell. 2019, 179(5): 1033–1055. https://doi.org/10.1016/j.cell.2019.10.017
Sun X, Malhotra A (2018) Noncoding RNAs (ncRNA) in Hepato Cancer: A Review. J Environ Pathol Toxicol Oncol. 2018, 37(1): 15–25. https://doi.org/10.1615/JEnvironPatholToxicolOncol.2018025223
Tan JQ, Li Z, Chen G et al (2022) The natural compound from Garcinia bracteata mainly induces GSDME-mediated pyroptosis in esophageal cancer cells. Phytomedicine. 2022, 102: 154142. https://doi.org/10.1016/j.phymed.2022.154142
Tang Q, Zheng X, Zhang J (2018) Long non-coding RNA CRNDE promotes heptaocellular carcinoma cell proliferation by regulating PI3K/Akt /beta-catenin signaling. Biomed Pharmacother. 2018, 103: 1187–1193. https://doi.org/10.1016/j.biopha.2018.04.128
Vergara IA, Erho N, Triche TJ et al (2012) Genomic Dark Matter in Prostate Cancer: Exploring the Clinical Utility of ncRNA as Biomarkers. Front Genet. 2012, 3: 23. https://doi.org/10.3389/fgene.2012.00023
Wang Y, Wang Y, Li J et al (2015) CRNDE, a long-noncoding RNA, promotes glioma cell growth and invasion through mTOR signaling. Cancer Lett. 2015, 367(2): 122–128. https://doi.org/10.1016/j.canlet.2015.03.027
Wang Q, Wang LX, Zhang CY et al (2022) LncRNA CRNDE promotes cell proliferation, migration and invasion of ovarian cancer via miR-423-5p/FSCN1 axis. Mol Cell Biochem. 2022, 477(5): 1477–1488. https://doi.org/10.1007/s11010-022-04382-8
Wang Y, Wang M, Chen J et al (2023) The gut microbiota reprograms intestinal lipid metabolism through long noncoding RNA Snhg9. Science. 2023, 381(6660): 851–857. https://doi.org/10.1126/science.ade0522
Wei X, Li Z, Zheng H et al (2024) Long non-coding RNA MAGEA4-AS1 binding to p53 enhances MK2 signaling pathway and promotes the proliferation and metastasis of oral squamous cell carcinoma. Funct Integr Genomics. 2024, 24(5): 158. https://doi.org/10.1007/s10142-024-01436-6
Wong HL, Tie J (2023) Low intensity treatment in metastatic colorectal cancer. Lancet Gastroenterol Hepatol. 2023, 8(2): 97–99. https://doi.org/10.1016/S2468-1253(22)00380-6
Yao H, Huang C, Zou J et al (2024) Extracellular vesicle-packaged lncRNA from cancer-associated fibroblasts promotes immune evasion by downregulating HLA-A in pancreatic cancer. Journal of extracellular vesicles. 2024 13(7): e12484. https://doi.org/10.1002/jev2.12484
Yu C, Xue J, Zhu W et al (2015) Warburg meets non-coding RNAs: the emerging role of ncRNA in regulating the glucose metabolism of cancer cells. Tumour Biol. 2015, 36(1): 81–94. https://doi.org/10.1007/s13277-014-2875-z
Yu Y, Wang L, Li Z et al (2021) Long noncoding RNA CRNDE functions as a diagnostic and prognostic biomarker in osteosarcoma, as well as promotes its progression via inhibition of miR-335-3p. J Biochem Mol Toxicol. 2021, 35(5): e22734. https://doi.org/10.1002/jbt.22734
Zhang T, Wu DM, Luo PW et al (2022) CircNEIL3 mediates pyroptosis to influence lung adenocarcinoma radiotherapy by upregulating PIF1 through miR-1184 inhibition. Cell Death Dis. 2022, 13(2): 167. https://doi.org/10.1038/s41419-022-04561-x
Zhong ME, Chen Y, Zhang G et al (2019) LncRNA H19 regulates PI3K-Akt signal pathway by functioning as a ceRNA and predicts poor prognosis in colorectal cancer: integrative analysis of dysregulated ncRNA-associated ceRNA network. Cancer Cell Int. 2019, 19: 148. https://doi.org/10.1186/s12935-019-0866-2
Zhu HY, Gao YJ, Wang Y et al (2021) LncRNA CRNDE promotes the progression and angiogenesis of pancreatic cancer via miR-451a/CDKN2D axis. Transl Oncol. 2021, 14(7): 101088. https://doi.org/10.1016/j.tranon.2021.101088
Zou H, Luo J, Guo Y et al (2024) Tyrosine phosphorylation-mediated YAP1-TFAP2A interactions coordinate transcription and trastuzumab resistance in HER2+breast cancer. Drug Resist Updat. 2024, 73: 101051. https://doi.org/10.1016/j.drup.2024.101051